Supporting. Information

Bandgap Engineering in Two-Dimensional Halide Perovskite $Cs_3Sb_2I_9$ Nanocrystals under Pressure

Ting Geng, Zhiwei Ma, Yaping Chen, Ye Cao, Pengfei Lv, Nan Li, and Guanjun Xiao*

State Key Laboratory of Superhard Materials, College of Physics, Jilin University Changchun 130012, China

+ These authors contributed equally to this work.

Corresponding Author: xguanjun@jlu.edu.cn

Experimental Section

Materials. All reagents were used as received without further purifications: Cs_2CO_3 (cesium carbonate, 99.9%, Alfa), SbI_3 (antimony(III) iodide, ultra dry, 99.998%, Alfa), OA (oleic acid, technical grade 90%, Sigma), OnA (octanoic acid, 99%, acros), OAm (Oleylamine, technical grade 70%, Sigma), ODE (1-Octadecene, technical grade 90%, Alfa), toluene (99.5%).

Preparation of Cs-oleate. The Cs-oleate was synthesized following a reported method.[1] 0.35 g (0.1 M) Cs_2CO_3, 20 mL ODE and 1.25 mL OA were taken in 50 mL 3-necked round bottom flask and the mixture was stirred under vacuum for 60 minutes at 120 °C for removal of O_2 and moisture from the reaction mixture. Then temperature of the reaction was raised to 150 °C to get a clear solution of Cs-oleate. The whole reaction process was carried out under the N_2 atmosphere. This Cs-oleate solution was stored at room temperature for further use.

Synthesis of $Cs_3Sb_2I_9$ nanocrystals. $Cs_3Sb_2I_9$ nanocrystals were synthesized by employing hot injection method. 50.2 mg (0.1 mmol) SbI_3 and 10 ml ODE were taken in a 50 mL 3-necked round bottom flask and 1 mL OnA and 0.4 mL OAm were added to the mixture degassed at 80 °C for 60 minutes along with magnetic stirring. Then the temperature was increased to 140 °C to dissolve SbI_3 and the reaction mixture became luminous yellow. The reaction mixture became orange when temperature was raised to 230 °C. After that pre-synthesized Cs-oleate (0.1 M, 0.3 mL), preheated at 100 °C, was swiftly injected to the reaction mixture at 230 °C. Within few seconds, the reaction mixture became turbid red and after 1 min the reaction was quenched by dipping the reaction flask into an ice bath. N_2 atmosphere was maintained throughout the reaction process. The synthesized $Cs_3Sb_2I_9$ nanocrystals were precipitated by centrifugation at 8000 rpm for 5 min, followed by re-dispersing the $Cs_3Sb_2I_9$ nanocrystals in toluene for further studies.

Characterization and High-Pressure Generation. The resulting samples were characterized by transmission electron microscopy (TEM) and high-resolution TEM performed on a JEM-2200FS with an emission gun operating at 200 kV. High-pressure experiments were carried out with a symmetric diamond anvil cell (DAC), and the culets size of the diamond anvils was 400 μm. The sample was loaded into a 130 μm-diameter chamber of the T301 stainless steel gasket pre-indented to a thickness of 40 μm. A small ruby ball was placed in the sample compartment for in situ pressure calibration. The pressure calibration was determined utilizing the standard ruby fluorescent technique.[2] In high-pressure experiments, silicon oil was utilized as the pressure transmitting medium (PTM) for in situ high-pressure optical absorption and XRD experiments, while the argon was employed as PTM for Raman measurements. These PTM did not have any detectable effect on the behavior of $Cs_3Sb_2I_9$ under pressure. All of the measurements were performed at room temperature.

Optical Measurements. In situ absorption photographs of the samples were obtained using a camera (Canon Eos 5Dmark II) equipped on a microscope (Ecilipse TI-U, Nikon). The camera can record the photographs under the same conditions including exposure time and intensity. In situ high-pressure optical absorption spectra measurements were carried out between 250 and 1000 nm using a deuterium-halogen light source and recorded with an optical fiber spectrometer (Ocean Optics, QE65000) with the data-collection time of 8 s. Each new acquisition was carried out several minutes later after elevation of the pressure, aiming to account for any kinetic dependence during measurements. In situ high pressure angle-dispersive X-ray diffraction (ADXRD) patterns were obtained with a wavelength of 0.6199 Å at beamline 15U1, Shanghai Synchrotron Radiation Facility (SSRF), China. CeO_2 was used as the standard sample to do the calibration. In situ high-pressure Raman spectra were recorded using a spectrometer equipped with liquid nitrogen cooled CCD (iHR 550, Symphony II, Horiba Jobin Yvon). A 785 nm single-mode DPSS laser was utilized to excite the sample, and the output power was 10 mW. The resolution of the system was 1 cm^{-1}. All the high-pressure experiments were performed at room temperature.

Refinements. Refinements of XRD patterns were accomplished using the Reflex module combined in Materials Studio 8.0 program. All refinements were performed using four refinement cycles fine convergence criteria. First, the pattern was indexed by means of the peak picking option of the software package. Then, a Pawle profile-fitting procedure was applied to refine cell parameters and search space group. The refinements were performed to obtain the crystal structural parameters. The quality of the fitting between the experimental and calculated profile is assessed by the various R parameters like Rp (profile factor) and Rwp (weighted profile factor).[3]

$$R_P = \left\{ \frac{\sum_i \left| I_i^{obs} - I_i^{cal} \right|}{\sum_i I_i^{obl}} \right\}$$

$$R_{\mathrm{wp}} = \left\{ \frac{\sum_i w_i \left(I_i^{obs} - I_i^{cal} \right)^2}{\sum_i w_i \left(I_i^{obs} \right)^2} \right\}^{\frac{1}{2}}$$

Where I_i^{obs} , I_i^{cal} and “i” indicate the experimental, calculated and total number of points respectively. And the “w_i” is the reciprocl of the variance of observation I_i^{obs} .

First-principles calculations. Calculations were performed within the framework of density functional theory (DFT) by using plane-wave pseudopotential methods. Geometry optimization was calculated using the plane-wave pseudopotential method with the generalized gradient approximation (GGA) based on density functional theory with CASTEP package. The plane-wave cutoff energy of 350 eV and Monkhorst-Pack grid for the electronic Brillouin zone integration was 5×5×3. The self-consistent field (SCF) tolerance was set as 1.0×10-6 eV/atom. The convergence thresholds between optimization cycles for maximum force, maximum stress and maximum displacement are set as 0.03 eV/Å, 0.05 GPa, and 1.0 ×10-3 Å, respectively. The partial density of states (DOSs) of isolated atoms were collected by adopting the identical pseudopotential of the GGA that is implemented in the Vienna ab initio simulation package (VASP).

References

(1) Q. Akkerman, S. Genaro Motti, A. Srimath Kandada, E. Mosconi, V. D'Innocenzo, G. Bertoni, S. Marras, B. A Kamino, L. Miranda, F. Angelis, A. Petrozza, M. Prato, L. Manna, J. Am. Chem. Soc. **2016,** *138*. 1010.

(2) H. K. Mao, J. Xu, P. M. Bell, J. *Geophys. Res.* **1986**, *91*, 4673.

(3) E. Jansen, W. Schafer, G. Will, J. *Appl. Crystallogr.* **1994**, *27*, 492.

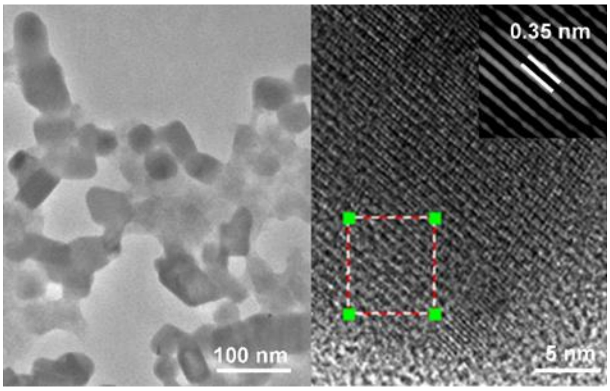

Fig. S1 TEM and HRTEM images of $Cs_3Sb_2I_9$ NCs.

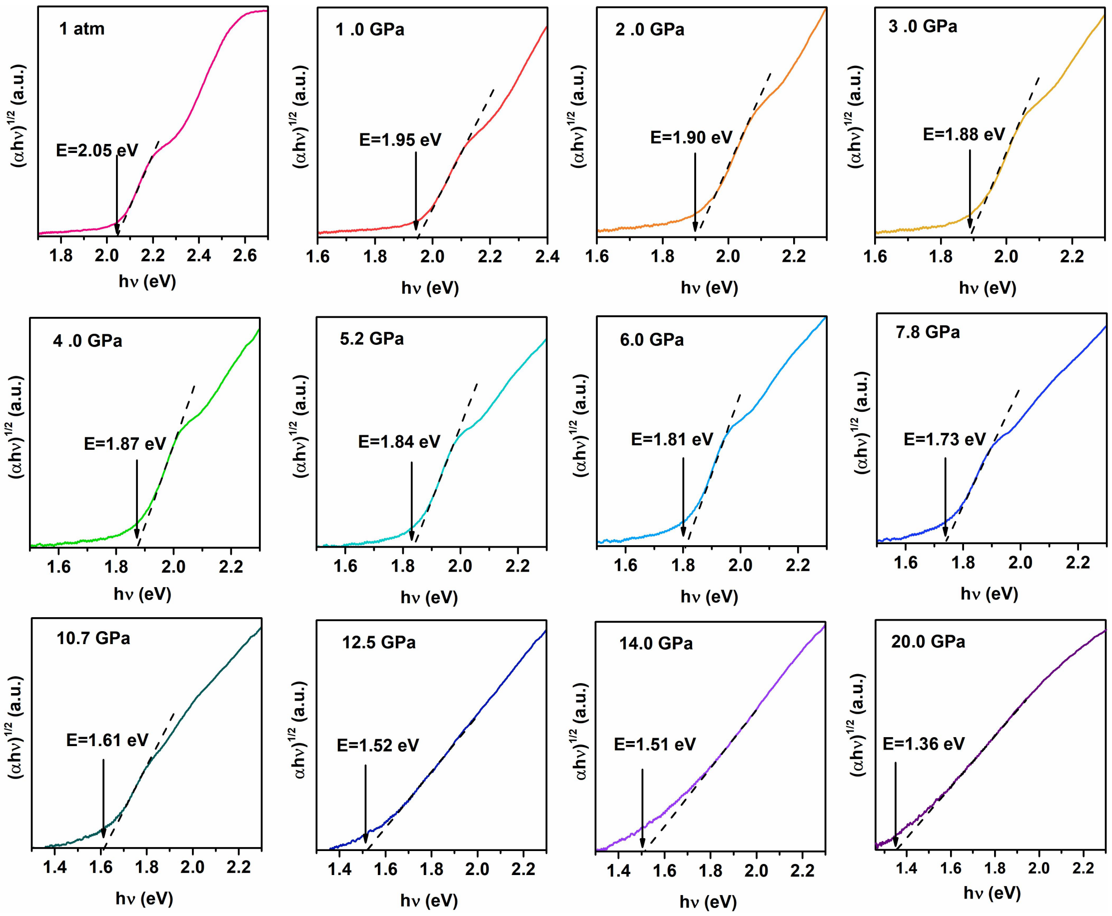

Fig. S2 High pressure analysis of Tauc plot of the absorbance data and the band gap value during compression.

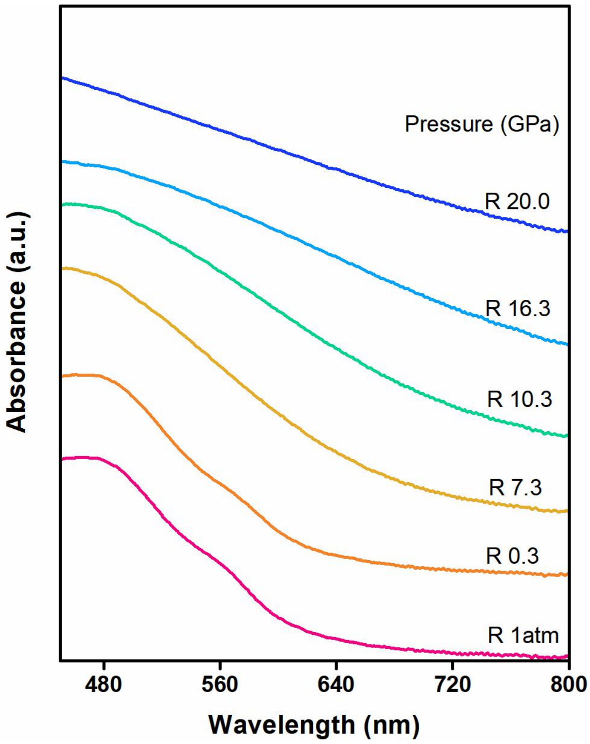

Fig. S3 In situ UV/vis absorption spectra of $Cs_3Sb_2I_9$ NCs upon the release of external pressure to the ambient environment.

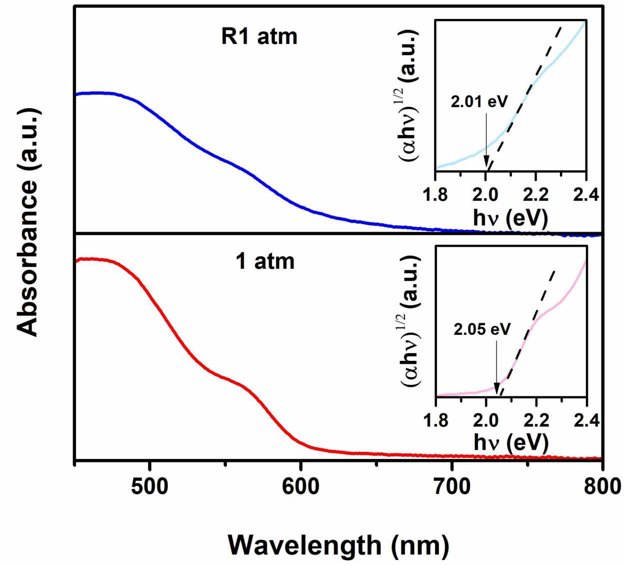

Fig. S4 UV/vis absorption spectra of the $Cs_3Sb_2I_9$ NCs at ambient conditions and decompression, respectively.

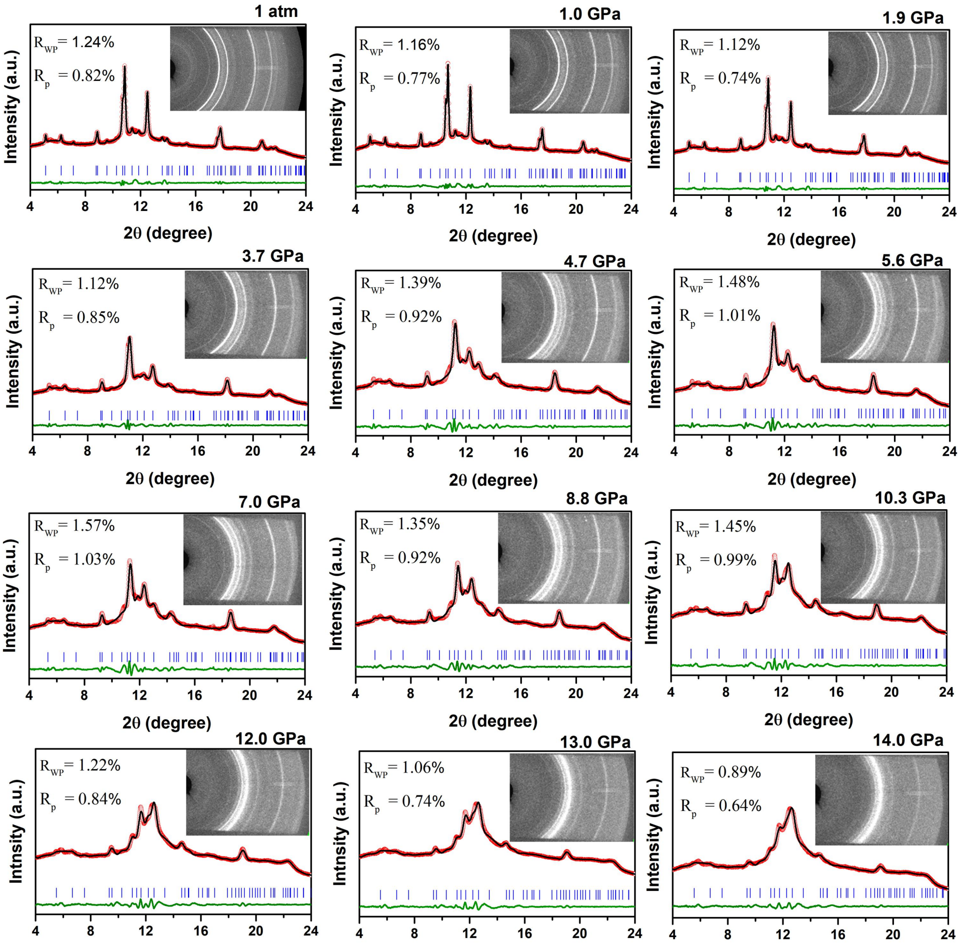

Fig. S5 Refinements of $Cs_3Sb_2I_9$ NCs at different pressures (Experimental: red circle; Simulation: black line; Bragg reflections: blue bar; Deviation: green line).

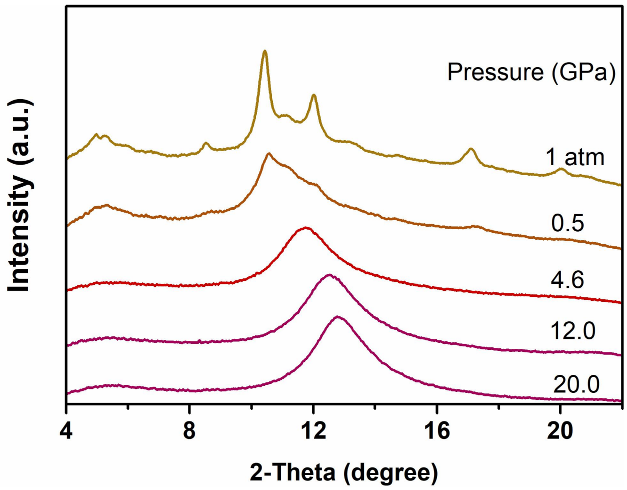

Fig. S6 Selected ADXRD patterns of $Cs_3Sb_2I_9$ NCs upon decompression.

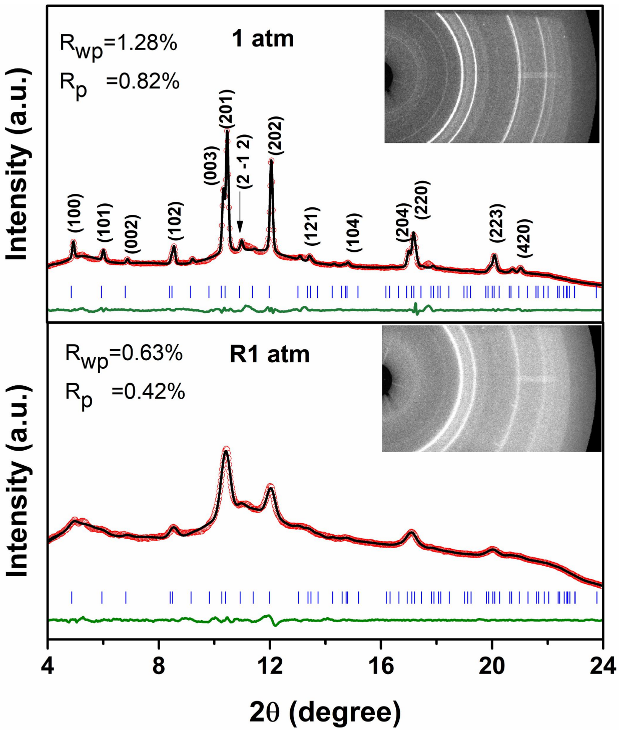

Fig. S7 Comparison between ADXRD spectra detected at1 atm and after releasing pressure to ambient conditions.

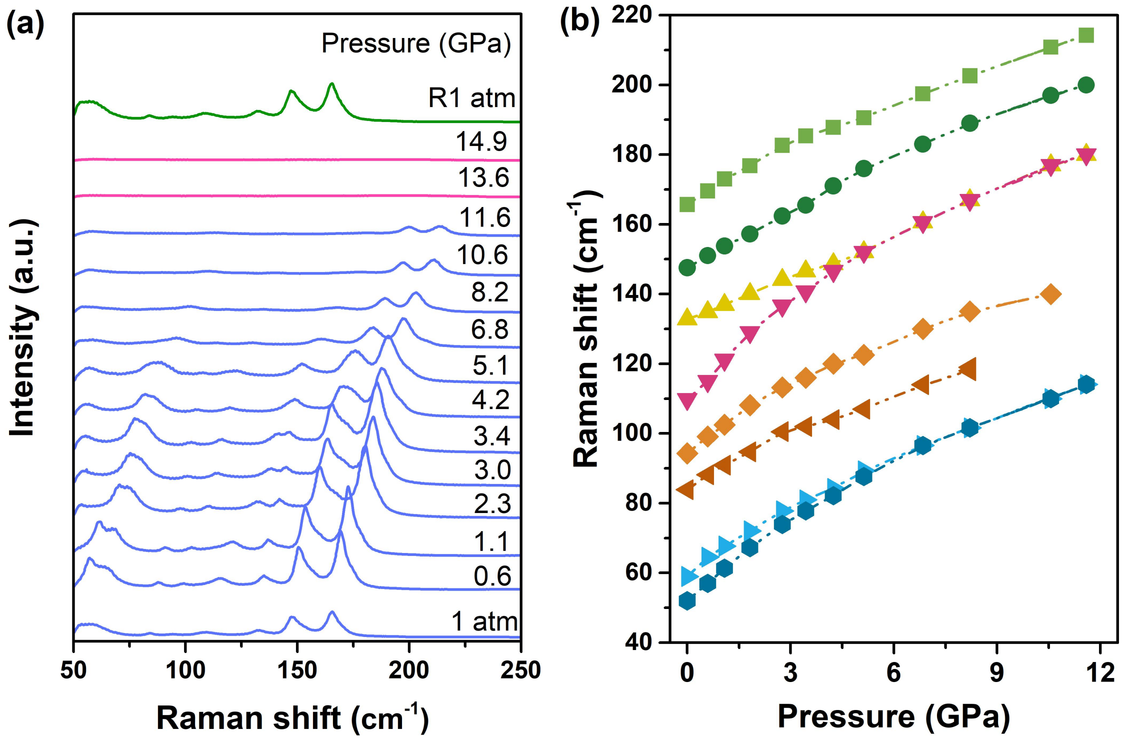

Fig. S8 a) Raman spectra of $Cs_3Sb_2I_9$ NCs as a function of pressure during compression and decompression at room temperature. b) Raman shift of $Cs_3Sb_2I_9$ NCs as a function of pressure.

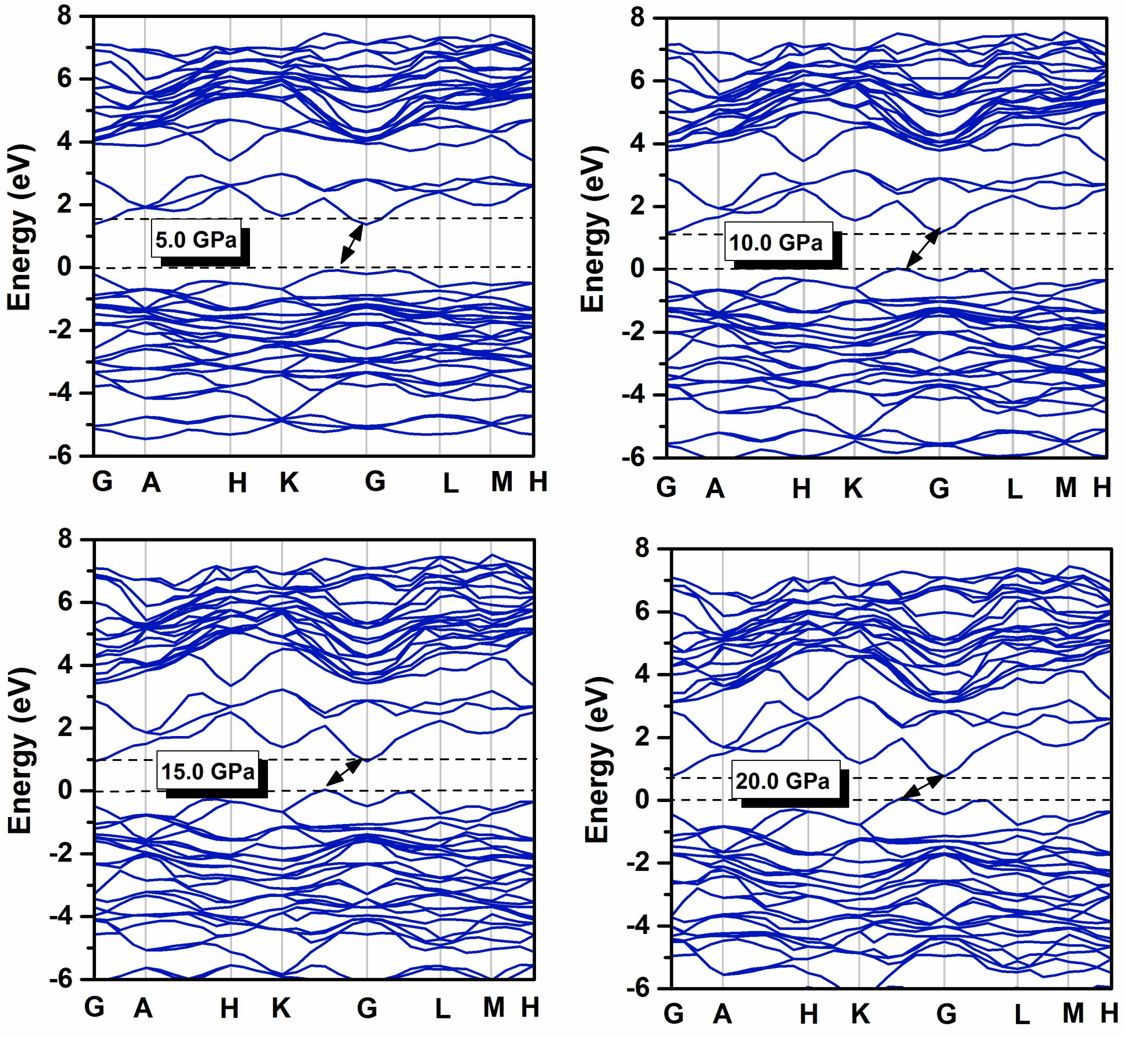

Fig. S9 Calculated electronic band structure of $Cs_3Sb_2I_9$ NCs at different pressure.

Table S1. Refined structural information of $Cs_3Sb_2I_9$ at 1 atm.

```
=============================================================
Lattice type               P

Space group name         P -3 m 1

Space group number      164

Setting number             1

Lattice parameters

       a                    b                 c              alpha           beta            gamma

  8.2971(0)          8.2971(0)       10.3145(0)       90.0000        90.0000        120.0000


Unit-cell volume = 614.9381(9) Å^3

=============================================================
```

.

Table S2. The corresponding refinement results Rwp and Rp.

Pressure (GPa)	**R_{wp} (%)**	**R_p (%)**
0.0	1.24	0.82
1.0	1.16	0.77
1.9	1.12	0.74
3.7	1.12	0.85
4.7	1.39	0.92
5.6	1.48	1.01
7.0	1.57	1.03
8.8	1.35	0.92
10.3	1.45	0.99
12.0	1.22	0.84
13.0	1.06	0.74
14.0	0.89	0.64

Table S3. The refinement Unit-cell volume and Lattice parameters at different pressures.

Pressure (GPa)	V (Å^3)	a=b (Å)	c (Å)
0.0	614.9381(9)	8.2971(0)	10.3145(0)
1.0	579.1959(4)	8.1303(0)	10.1177(0)
1.9	554.1030(1)	8.0110(0)	9.9698(0)
3.7	523.0605(5)	7.8564(0)	9.7853(0)
4.7	511.9281(3)	7.7932(0)	9.7330(0)
5.6	501.6550(3)	7.7415(0)	9.6655(0)
7.0	488.5377(9)	7.6636(0)	9.6051(0)
8.8	477.2048(2)	7.5974(0)	9.5465(0)
10.3	464.7130(4)	7.5226(0)	9.4824(0)
12.0	453.2483(5)	7.4532(0)	9.4215(0)
13.0	447.0159(3)	7.4145(0)	9.3892(0)
14.0	443.2139(3)	7.3879(0)	9.3765(0)

Table S4. The Sb-I bonds and I-Sb-I angles within antimony-iodide octahedron for $Cs_3Sb_2I_9$ NCs as function of pressure.

Pressure (GPa)	**I_1-Sb-I_1 angles (degree)**	**I_2-Sb-I_2 angles (degree)**	**Sb-I_1 bonds length L_1 (Å)**	**Sb-I_2 bonds length L_2 (Å)**
0.0	83.089(3)	95.603(1)	3.1276(6)	2.8279(6)
1.0	83.045(4)	95.567(7)	3.0661(1)	2.7718(8)
1.9	83.043(1)	95.565(8)	3.0211(9)	2.7312(5)
3.7	83.009(1)	95.538(4)	2.9638(8)	2.6791(3)
4.7	82.954(8)	95.446(0)	2.9133(5)	2.6595(2)
5.6	82.907(6)	95.456(3)	2.9234(6)	2.6416(6)
7.0	82.745(7)	95.325(2)	2.8986(8)	2.6178(0)
8.8	82.637(9)	95.237(9)	2.8767(1)	2.5969(9)
10.3	82.504(7)	95.129(7)	2.8521(7)	2.5736(4)
12.0	82.385(2)	95.032(7)	2.8292(2)	2.5518(8)
13.0	82.310(3)	94.971(7)	2.8166(3)	2.5398(7)
14.0	82.215(4)	94.894(4)	2.8091(9)	2.5323(2)

*The specific location of bond lengths and bond angles in the crystal structure has been marked in Fig. 4e.